

Dihydrogen versus Dihydride: Relativistic Effects on the Relative Stabilities of Nonclassical and Classical Isomers of $M(\text{PH}_3)_3\text{H}_4$ ($M = \text{Fe}, \text{Ru}, \text{Os}$)

Jian Li, Ross M. Dickson, and Tom Ziegler*

Contribution from the Department of Chemistry, University of Calgary, Calgary, Alberta, Canada T2N 1N4

Received December 28, 1994[®]

Abstract: A nonlocal, quasirelativistic density functional method, NL-SCF+QR, has been used to study the geometries and relative stabilities of the classical (I) and nonclassical (II) isomers of $M(\text{PH}_3)_3\text{H}_4$ with $M = \text{Fe}, \text{Ru},$ and Os . According to the energy calculations based on optimized geometries, the dihydrogen complex (II) is found to be most stable for Fe and Ru whereas the hydride complex (I) is the isomer of lowest energy for Os. These findings are in accordance with experimental observations. It was further found that relativistic effects are responsible for the changeover in the order of stability between I and II in going from $M = \text{Fe}$ and Ru to $M = \text{Os}$. Without relativity all three metal centers would prefer conformation II. The observed preference for a dihydride complex (I) in the case of the heavier congener osmium is explained by a relativistic destabilization of the 5d orbital which makes the metal center more basic.

I. Introduction

Dihydrogen complexes in which H_2 is coordinated through both hydrogens to a metal center were discovered by Kubas¹ and co-workers. They are now part of a growing class of compounds in which an electron pair in a σ -bond donates parts of its electron density to the metal. Other members of the family are so-called agostic complexes² in which a C–H bond is coordinated to a metal center primarily through hydrogen. The σ -complexes complement³ Werner-type compounds where a ligand donates electron density through its lone pair(s), e.g., NH_3 , and π -complexes such as Zeise's salt in which density is donated from the π -orbital. Dihydrogen can in addition act as a σ^* -acceptor through its antibonding and vacant σ^* orbital, and forms in this regard a counterpart to classical π^* -acceptor ligands such as CO and ethylene.

Dihydrogen complexes are valence tautomers with dihydrides formed from oxidative addition of H_2 to a metal center, and the relative stability of the $M\text{--H}_2$ and H--M--H bonding modes⁴ depends on a fine balance between the donor and acceptor properties of the metal center. The bonding in $M\text{--H}_2$ and H--M--H complexes has been the subject of several ab initio studies.⁵

Usually, the energy difference between the nonclassical, $M\text{--H}_2$, and classical, H--M--H , hydride isomers is rather small. An experimental estimate based on NMR techniques suggests that the nonclassical isomer of $\text{W}(\text{PR}_3)_2(\text{CO})_3(\text{H}_2)$ is only about 1 kcal/mol more stable than the corresponding classical tautomer.⁶ Many factors can affect the relative stabilities, such as

variations in the ancillary ligands, the introduction of a total charge for the complex, trans or cis ligand effects, and the replacement of one metal center by other.

Concerning the nature of the metal center, one interesting observation is that in the iron triad, $\text{Fe}(\text{PR}_3)_3\text{H}_4$ and $\text{Ru}(\text{PR}_3)_3\text{H}_4$ are nonclassical dihydrogen complexes while the heavier congener $\text{Os}(\text{PR}_3)_3\text{H}_4$ is a classical hydride.⁷ Since relativity plays an increasing role from the top toward the bottom of a transition metal triad,⁸ it can be expected that the trend mentioned above might be influenced by relativistic effects.

We have recently found⁹ that relativistic effects enhance the strength in bonds between π -ligands¹⁰ such as CO, O_2 , C_2H_4 , or C_2H_2 and third-row transition metal centers. A detailed

(5) (a) Hay, P. J. *Chem. Phys. Lett.* **1984**, *103*, 466. (b) Hay, P. J. *J. Am. Chem. Soc.* **1987**, *109*, 705. (c) Kober, E. M.; Hay, P. J. In *The challenge of d and f elements, theory and computation*; ACS Symposium Series 394; Salahub, D. R., Zerner, M. C., Eds.; American Chemical Society: Washington, DC, 1989. (d) Haynes, G. R.; Martin, R. L.; Hay, P. J. *J. Am. Chem. Soc.* **1992**, *114*, 28. (e) Lin, Z.; Hall, M. B. *Inorg. Chem.* **1991**, *30*, 2569. (f) Lin, Z.; Hall, M. B. *J. Am. Chem. Soc.* **1992**, *114*, 2928. (g) Lin, Z.; Hall, M. B. *J. Am. Chem. Soc.* **1992**, *114*, 6102. (h) Lin, Z.; Hall, M. B. *Inorg. Chem.* **1992**, *31*, 4262. (i) Lin, Z.; Hall, M. B. *Organometallics* **1992**, *11*, 3801. (j) Lin, Z.; Hall, M. B. *Organometallics* **1993**, *12*, 4046. (k) Lin, Z.; Hall, M. B. *J. Am. Chem. Soc.* **1994**, *116*, 4446. (l) Sargent, A. L.; Hall, M. B.; Guest, M. F. *J. Am. Chem. Soc.* **1992**, *114*, 517. (m) Sargent, A. L.; Hall, M. C. *Inorg. Chem.* **1992**, *31*, 317. (n) Maseras, F.; Duran, M.; Lledos, A.; Bertran, J. *J. Am. Chem. Soc.* **1991**, *113*, 2879. (o) Maseras, F.; Koga, N.; Morokuma, K. *J. Am. Chem. Soc.* **1993**, *115*, 8313. (p) Maseras, F.; Li, X.-K.; Koga, N.; Morokuma, K. *J. Am. Chem. Soc.* **1993**, *115*, 10974. (q) Pacchioni, G. *J. Am. Chem. Soc.* **1990**, *112*, 80. (r) Pacchioni, G.; Bagus, P. S. *Rend. Lincei. Sci. Nat.* **1991**, *2*, 3. (s) Craw, J. S.; Bacskey, G. B.; Hush, N. S. *J. Am. Chem. Soc.* **1994**, *116*, 5937.

(6) Khalsa, G. R. K.; Kubas, G. J.; Unkefer, C. J.; Van der Sluys, L. S.; Kubat-Martin, K. A. *J. Am. Chem. Soc.* **1990**, *112*, 3855.

(7) (a) Crabtree, R. H.; Hamilton, D. G. *J. Am. Chem. Soc.* **1986**, *108*, 3124. (b) Van der Sluys, L. S.; Eckert, J.; Eisenstein, O.; Hall, J. H.; Huffman, J. C.; Jackson, S. A.; Koetzle, T. F.; Kubas, G. J.; Vergamini, P. J.; Caulton, K. G. *J. Am. Chem. Soc.* **1990**, *112*, 4831. (c) Hart, D. W.; Bau, R.; Koetzle, T. F. *J. Am. Chem. Soc.* **1977**, *99*, 7557.

(8) Pyykkö, P. *Chem. Rev.* **1988**, *88*, 563.

(9) (a) Li, J.; Schreckenbach, G.; Ziegler, T. *J. Phys. Chem.* **1994**, *98*, 4838. (b) Li, J.; Schreckenbach, G.; Ziegler, T. *J. Am. Chem. Soc.* **1994**, in press. (c) Li, J.; Schreckenbach, G.; Ziegler, T. *Inorg. Chem.* **1995**, *34*, 3245.

(10) (a) Dewar, M. J. S. *Bull. Soc. Chim. Fr.* **1951**, *18*, C79. (b) Chatt, J.; Duncanson, L. A. *J. Chem. Soc.* **1953**, 2339.

[®] Abstract published in *Advance ACS Abstracts*, November 15, 1995.

(1) (a) Kubas, G. J.; Ryan, R. R.; Swanson, B. J.; Vergamini, P. J.; Wasserman, H. J. *J. Am. Chem. Soc.* **1984**, *106*, 451. (b) Kubas, G. J.; Ryan, R. R.; Wroblewski, D. *J. Am. Chem. Soc.* **1986**, *108*, 1339. (c) Kubas, G. J. *Acc. Chem. Res.* **1988**, *21*, 120. (d) Kubas, G. J. *Comments Inorg. Chem.* **1988**, *7*, 17. (e) Heinekey, D. M.; Oldham, W. J., Jr. *Chem. Rev.* **1993**, *93*, 913.

(2) (a) Brookhart, M.; Green, M. L. H. *J. Organomet. Chem.* **1983**, *250*, 395. (b) Brookhart, M.; Green, M. L. H.; Wang, L. L. *Prog. Inorg. Chem.* **1988**, *36*, 1.

(3) (a) Crabtree, R. H.; Hamilton, D. G. *Adv. Organomet. Chem.* **1988**, *28*, 299. (b) Crabtree, R. H. *Angew. Chem., Int. Ed. Engl.* **1993**, *32*, 789.

(4) Morris, J. H.; Jessop, P. G. *Coord. Chem. Rev.* **1992**, *121*, 155.

analysis indicates that the relativistic effects strengthen the metal–ligand bonds by increasing the metal to ligand back donation.¹⁰ This increase is the result of a relativistic destabilization⁹ of the metal d orbitals which diminishes the energy gap to the π^* -acceptor orbitals on the ligands.

As already mentioned, dihydrogen is a σ -donor as well as a σ^* -acceptor,¹¹ and we shall in the present study examine how the relative strengths of the two bonding modes change within the series $M(\text{PH}_3)_3\text{H}_4$ with $M = \text{Fe}, \text{Ru}, \text{Os}$, and how any such change will influence the relative stabilities of the nonclassical and classical isomers of $M(\text{PH}_3)_3\text{H}_4$. Of particular interest will be the role played by relativity. In addition, we also want to demonstrate that density functional theory¹² is a suitable method for studies of the geometries and energetics of metal hydride complexes.

II. Computational Details

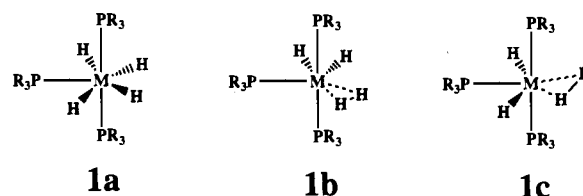
The calculations reported here were carried out using the density functional package, ADF, developed by Baerends *et al.*,¹³ and vectorized by Ravenek.¹⁴ The adopted numerical integration scheme was that developed by te Velde *et al.*¹⁵ A set of uncontracted triple- ζ Slater-type orbitals (STO) was employed for the $ns, np, nd, (n+1)s$, and $(n+1)p$ valence orbitals of the transition metal atoms.¹⁶ For the 3s and 3p orbitals of phosphorus, use was made of a double- ζ basis augmented by an extra d polarization function. For the hydrogen atoms on phosphorus the basis was of double- ζ quality with one additional p polarization function. The hydrogens bound to the metal center had a triple- ζ 1s basis with one p function added. The inner core shells were treated by the frozen-core approximation.¹³ A set of auxiliary s, p, d, f, and g STO functions, centered on all nuclei, was introduced to fit the molecular density and to represent Coulomb and exchange potentials accurately.¹⁷ All molecular geometries were optimized according to the analytical energy gradient method implemented by Versluis and Ziegler¹⁸ at the LDA level¹⁹ and by Fan and Ziegler²⁰ at the nonlocal (NL) level, NL-SCF. The NL corrections adopted were based on Beckes's functional for exchange²¹ and Perdew's functional for correlation.²²

The relativistic effects were taken into account at two levels of theory. In the lower level scheme based on first-order perturbation theory (FO),²³ terms up to first order in α^2 (α is the fine structure constant) are retained in the Hamiltonian as a perturbation, and therefore, the energy of the molecule includes contributions from the mass-velocity, Darwin, and spin–orbit terms.²³ In the more elaborate quasirelativistic method (QR)²⁴ changes in the density induced by the

first-order Hamiltonian are taken into account to all orders of α^2 whereas operators in the Hamiltonian to second and higher orders are neglected. The QR scheme can readily be extended to include energy gradients of importance for structure optimizations.²⁵ The scheme in which both nonlocal and quasirelativistic corrections are taken into account self-consistently will be referred to as NL-SCF+QR.

III. Results and Discussion

Geometrical Optimization of Classical and Nonclassical Structures. The structures of $\text{Fe}(\text{PR}_3)_3\text{H}_4$ and $\text{Os}(\text{PR}_3)_3\text{H}_4$ have been determined by neutron diffraction methods.^{7b,c} The three phosphines are arranged in a mer conformation and the four hydrogens are roughly in a plane perpendicular to that of the phosphorus atoms, as illustrated in **1a** for the classical hydride $\text{Os}(\text{PR}_3)_3\text{H}_4$ and in **1b** for the corresponding nonclassical dihydrogen complex $\text{Fe}(\text{PR}_3)_3\text{H}_4$. We shall in addition to the observed dihydrogen conformation **1b** also consider **1c** in which the H_2 ligand is trans to a phosphine rather than a hydride as in **1b**.



All geometries have been optimized using a C_s constraint with all hydrogens in the symmetry plane at the LDA, NL-SCF, and NL-SCF+QR levels of theory. Selected NL-SCF+QR geometrical parameters related to the M–H and H–H bonds are shown in Figure 1. In Table 1 and 2, we compare the optimized geometries for the Fe and Os complexes with the experimental structures of $\text{Fe}(\text{PEtPh}_2)_3(\text{H}_2)\text{H}_2$ ^{7b} and $\text{Os}(\text{PMe}_2\text{Ph})_3\text{H}_4$.^{7c}

It follows from Tables 1 and 2 that the geometries optimized at the highest level of theory, NL-SCF+QR, are in reasonable agreement with the experimental structures. Although we replace the substituted phosphine ligands PEtPh_2 and PMe_2Ph with PH_3 , the calculated Fe–P and Os–P bond lengths compare well with the experimental ones. However, as expected, the steric bulk of the substituted phosphine ligands cannot be easily simulated by PH_3 , so that the calculated P–M–H or P–M–P angles are smaller than the observed values. The Fe–H and Os–H distances are reproduced at remarkably high accuracy with a deviation about 0.01–0.02 Å. The calculated Fe–H₃ or Fe–H₄ distances are significantly longer than Fe–H₁ or Fe–H₂ bonds, in accordance with the experimental observation. The largest disparity occurs in the dihydrogen iron complex where the calculated H1–H2 bond length is about 0.12 Å longer than the experimental one.

Maseras *et al.* optimized the geometries of $\text{Os}(\text{PH}_3)_3\text{H}_4$ at the restricted Hartree–Fock (RHF) level where electron correlation is neglected. Optimizations were also carried out using second-order Møller–Plesset perturbation theory (MP2) which includes some correlation. All the ab initio calculations made use of relativistic effective core potentials.^{5p} The MP2 geometrical parameters for isomer **1a** are compared in Table 2 to our results and experiment. In general, the MP2 Os–P bond lengths are longer than experimental estimates and those obtained by the NL-SCF+QR scheme. On the other hand, the MP2 Os–H bond distances are shorter than the experimental values and those calculated by the NL-SCF+QR scheme.

(25) Schreckenbach, G.; Ziegler, T.; Li, J. *Int. J. Quantum Chem.* **1994**, in press.

(11) (a) Saillard, J.; Hoffmann, R. *J. Am. Chem. Soc.* **1984**, *106*, 2006. (b) Jean, Y.; Lledos, A.; Maouche, B.; Aiad, R. *J. Chim. Phys.* **1987**, *84*, 806. (c) Volatron, F.; Jean, Y.; Lledos, A. *New J. Chem.* **1987**, *11*, 651.

(12) (a) Parr, R. G.; Yang, W. *Density Functional Theory of Atoms and Molecules*, Oxford University Press: New York, 1988. (b) Labanowski, J.; Andzelm, J. *Density Functional Methods in Chemistry*; Springer-Verlag: Heidelberg, 1991. (c) Ziegler, T. *Chem. Rev.* **1991**, *91*, 651.

(13) Baerends, E. J.; Ellis, D. E.; Ros, P. *Chem. Phys.* **1973**, *2*, 41.

(14) Ravenek, W. In *Algorithms and applications on vector and parallel computers*; te Riele, H. J. J., Dekkar, Th. J., van de Vorst, H. A., Eds.; Elsevier: Amsterdam, 1987.

(15) (a) Boerrigter, P. M.; te Velde, G.; Baerends, E. J. *Int. J. Quantum Chem.* **1988**, *33*, 87. (b) te Velde, G.; Baerends, E. J. *J. Comput. Phys.* **1992**, *99*, 84.

(16) (a) Snijders, J. G.; Baerends, E. J.; Vernooijs, P. *At. Nucl. Data Tables* **1982**, *26*, 483. (b) Vernooijs, P.; Snijders, J. G.; Baerends, E. J. *Slater type basis functions for the whole periodic system*; Internal report, Free University of Amsterdam, The Netherlands, 1981.

(17) Krijn, J.; Baerends, E. J. *Fit functions in the HFS-method*; Internal Report (in Dutch), University of Amsterdam, The Netherlands, 1984.

(18) Versluis, L.; Ziegler, T. *J. Chem. Phys.* **1988**, *88*, 322.

(19) Vosko, S. H.; Wilk, L.; Nusair, M. *Can. J. Phys.* **1980**, *58*, 1200.

(20) Fan, L.; Ziegler, T. *J. Chem. Phys.* **1991**, *95*, 7401.

(21) Becke, A. *Phys. Rev. A* **1988**, *38*, 3098.

(22) Perdew, J. P. *Phys. Rev. B* **1986**, *33*, 8822. Erratum: *Phys. Rev. B* **1986**, *34*, 7406.

(23) (a) Snijders, J. G.; Baerends, E. J. *Mol. Phys.* **1978**, *36*, 1789. (b) Snijders, J. G.; Baerends, E. J.; Ros, P. *Mol. Phys.* **1979**, *38*, 1909.

(24) Ziegler, T.; Tschinke, V.; Baerends, E. J.; Snijders, J. G.; Ravenek, W. *J. Phys. Chem.* **1989**, *93*, 3050.

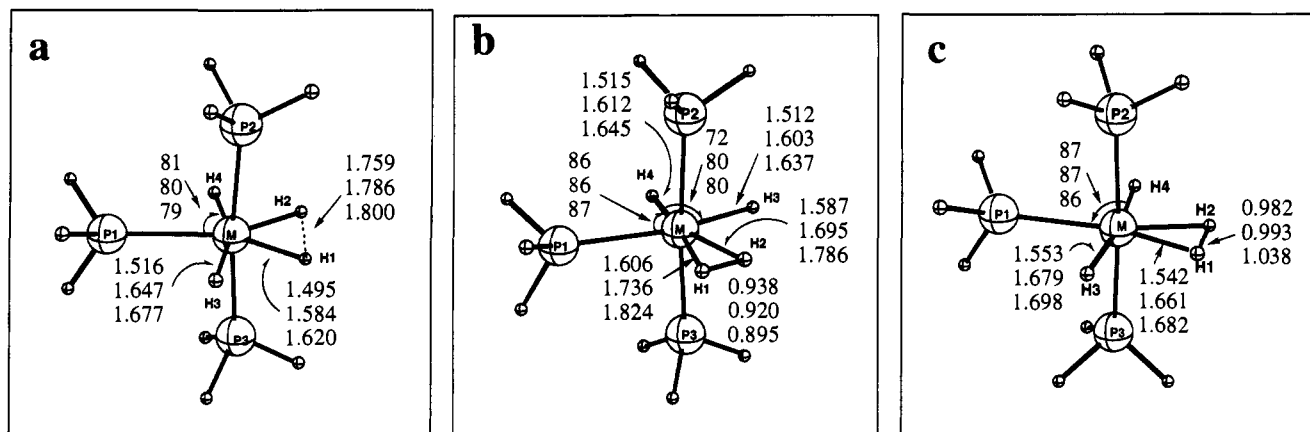


Figure 1. Three isomer structures of $M(\text{PH}_3)_3\text{H}_4$: (a) **1a**; (b) **1b**; (c) **1c**. Selected optimized geometrical parameters evaluated by the NL-SCF+QR scheme are shown too. For every triad, the data from top to bottom correspond to Fe, Ru, and Os complexes, respectively. Distances in Å angles in deg.

Table 1. Selected Geometrical Parameters for $\text{Fe}(\text{PH}_3)_3(\text{H}_4)^a$

	NL-SCF+QR	exp ^b
Fe-P1	2.194	2.206
Fe-P2	2.176	2.174
Fe-P3	2.176	2.162
Fe-H1	1.606	1.607
Fe-H2	1.587	1.576
Fe-H3	1.512	1.514
Fe-H4	1.515	1.538
H1-H2	0.938	0.821
P1-Fe-H1	77	82.4
P1-Fe-H4	86	93.9
H3-Fe-H4	77	88.2

^a Bond lengths in angstroms and bond angles in degrees. ^b Reference 7b.

Table 2. Selected Geometrical Parameters for $\text{Os}(\text{PH}_3)_3(\text{H}_4)^a$

	NL-SCF	NL-SCF+QR	MP2 ^b	exp ^c
Os-P1	2.487	2.375	2.412	2.347
Os-P2	2.402	2.306	2.342	2.307-2.317
Os-H1	1.630	1.620	1.608	1.644-1.648
Os-H3	1.718	1.677	1.649	1.663-1.681
H1-H2	1.786	1.800	1.759	1.840
P1-Os-H1	80	79	78.4	73.0-79.7
H1-Os-H3	67	67	69.7	69.4-70.0
P2-Os-P1	92	93	95.6	96.9-97.1

^a Bond lengths in angstroms and bond angles in degrees. ^b Reference 5p. ^c Reference 7c.

Table 3. Relative Energies^a (kcal/mol) for the Nonclassical, **1b** and **1c**, as well as Classical, **1a**, Isomers of $M(\text{PH}_3)_3\text{H}_4$

method	$\text{Fe}(\text{PH}_3)_3\text{H}_4$			$\text{Ru}(\text{PH}_3)_3\text{H}_4$			$\text{Os}(\text{PH}_3)_3\text{H}_4$		
	1a	1c	1b	1a	1c	1b	1a	1c	1b
LDA	0.1	2.5	0.0	1.6	5.9	0.0	4.3	3.3	0.0
LDA/NL	1.2	3.9	0.0	3.1	7.7	0.0	6.0	4.6	0.0
LDA/NL+FO	0.6	3.6	0.0	0.5	6.7	0.0	0.0	5.6	2.4
NL-SCF	2.4	3.7	0.0	3.9	7.7	0.0	6.5	6.2	0.0
NL-SCF/FO	0.9	3.4	0.0	0.4	5.9	0.0	0.0	7.4	1.5
NL-SCF+QR	0.8	3.4	0.0	1.2	6.1	0.0	0.0	10.6	4.2

^a The energy of the most stable conformation is set to zero for any given method or metal.

Relative Stabilities of Nonclassical and Classical Isomers.

Table 3 displays relative energies for the three isomers **1a**, **1b**, and **1c** at various levels of theory. The first entry, LDA, affords estimates based on the local method. The next two rows correspond to LDA geometries where energy differences have been evaluated by adding nonlocal, LDA/NL, and relativistic effects, LDA/NL+FO, as perturbations based on LDA densities.

Also shown are results in which nonlocal energies and geometries are calculated self-consistently without, NL-SCF, or with, NL-SCF/FO, relativity added as a perturbation. We have finally at the highest level, NL-SCF+QR, included nonlocal and relativistic effects self-consistently in the geometry optimizations and energy calculations.

It follows from Table 3 that the nonclassical dihydrogen isomer **1b** of $M(\text{PR}_3)_3\text{H}_4$ is the most stable conformation at all the calculated levels for $M = \text{Fe}$ and Ru. However, the classical hydride isomer, **1a**, is only slightly higher in energy. Our findings are in line with the experimental observation based on neutron diffraction for $\text{Fe}(\text{PEtPh}_2)_3(\text{H}_2)_2$ ^{7b} and NMR T_1 measurements^{7a} for $\text{Fe}(\text{PR}_3)_3\text{H}_4$ and $\text{Ru}(\text{PH}_3)_3\text{H}_4$.

In the case of the corresponding osmium complex, it seems that relativistic effects play a critical role for the relative stability of **1a** and **1b**. At the non-relativistic levels, LDA, LDA/NL, and NL-SCF, the nonclassical dihydrogen isomer **1a** is calculated to be most stable. This trend is reversed when relativistic effects are taken into account. At all three relativistic levels, LDA/NL+FO, NL-SCF/FO, and NL-SCF+QR, the most stable conformation is the classical hydride isomer **1b**, in accord with a structure determined by neutron diffraction.^{7c}

In general, relativity is seen to aid the classical hydride conformations **1a** compared to the nonclassical dihydrogen complex **1b**. Thus, relativity reduces the stability of **1b** compared to **1a** from 2.4 (NL-SCF) to 0.8 kcal/mol (NL-SCF+QR) in the case of iron, and from 3.9 (NL-SCF) to 1.2 kcal/mol (NL-SCF+QR) in the case of ruthenium. For the osmium complex, the **1b** isomer is 6.5 kcal/mol more stable than **1a** at the nonrelativistic NL-SCF level, whereas **1a** is 4.2 kcal/mol more stable than **1b** at the NL-SCF+QR level. It is interesting to note that the nonrelativistic stability of **1b** compared to **1a** increase from the top downward within the iron triad. We shall analyze how this trend is reversed by relativity in the next section.

The alternative nonclassical dihydrogen isomer, **1c**, is uniformly the most unstable of the three conformations studied here. It is likely less stable than the alternative dihydrogen isomer, **1b**, on account of the fact that it has the two hydrides trans to each other rather than cis as in **1b**. It has been estimated that cis is favored over trans by 10-20 kcal/mol.^{5g}

Lin and Hall have investigated the relative stability of the conformations **1a** to **1c** for the $\text{Ru}(\text{PH}_3)_3\text{H}_4$ and $\text{Os}(\text{PH}_3)_3\text{H}_4$ complexes by MP2 energy calculations based on HF geometries^{5g} and effective core potentials in which relativistic effects are included. They have not carried out purely nonrelativistic

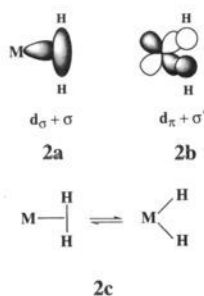
Table 4. Decomposition of the M–H₂ Interaction Energies^a

		$-E_{\text{steric}}$	$-E_{\text{D}}$	$-E_{\text{BD}}$	$-E_{\text{syn}}$	$-E_{\text{res}}$	$-E_{\text{prep}}$	ΔE^b	$D(\text{M}-\text{H})_{\text{av}}^c$
Fe(PH ₃) ₃ H ₄ (relativistic)	1a	-22.9	35.3	56.6	19.6	29.7	-93.2	25.1	69.0
	1c	-22.3	19.3	15.8	10.7	22.3	-23.3	22.5	
	1b	-19.5	13.8	13.4	10.2	26.0	-18.0	25.9	
Ru(PH ₃) ₃ H ₄ (relativistic)	1a	-22.6	31.6	61.9	16.8	34.6	-92.3	30.0	71.5
	1c	-20.0	16.7	15.6	10.9	24.4	-22.5	25.1	
	1b	-18.8	12.3	14.2	11.7	28.5	-16.7	31.2	
Os(PH ₃) ₃ H ₄ (nonrelativistic)	1a	-22.5	28.3	63.2	15.0	31.2	-98.9	16.3	64.6
	1c	-27.7	17.7	20.5	7.6	22.9	-24.4	16.6	
	1b	-24.7	12.1	10.8	9.5	32.7	-17.6	22.8	
Os(PH ₃) ₃ H ₄ (relativistic)	1a	-16.9	26.1	73.4	16.7	35.2	-103.1	31.4	72.2
	1c	-24.0	16.0	26.6	8.2	23.8	-29.8	20.8	
	1b	-20.6	10.5	15.5	9.8	31.1	-19.1	27.2	

^a Energies in kcal/mol. ^b Total bond energy is calculated according to eq 1 as $\Delta E = -[E_{\text{D}} + E_{\text{BD}} + E_{\text{syn}} + E_{\text{res}} + E_{\text{steric}} + E_{\text{prep}}]$. ^c $D(\text{M}-\text{H})_{\text{av}}$ is the average M–H dissociation energy in the classical dihydride **1a**. The electronic dissociation energy of H₂ was calculated as 112.9 kcal/mol at the NL-SCF level.

calculations for comparison. Lin and Hall found the classical dihydride conformation **1a** to be more stable than the dihydrogen isomer **1b** for ruthenium (3.3 kcal/mol) as well as osmium (13.6 kcal/mol), in disagreement with experiment. Maseras *et al.*^{5p} calculated conformation **1a** to be more stable than **1b** by 6.2, 15.0, 14.4, and 12.4 kcal/mol at HF, MP2, MP3, and MP4 levels in the case of Os(PH₃)₃H₄. The relative energies of **1a** and **1b** for the 4d and 3d congeners were not considered by Maseras *et al.*^{5p} It seems that the present DFT theory, NL-SCF+QR, is the first high-level theory which is able to account for the fine balance between **1a** and **1b** within the entire iron triad.

An Analysis of the M–H₂ Interaction Based on the Extended Transition State (EST) Energy Decomposition Scheme. As mentioned previously, the accepted description of the metal–dihydrogen bonding is based on the Dewar–Chatt–Duncanson model.¹¹ The primary interaction is believed to be a donation, **2a**, of electron density from the dihydrogen σ orbital to an empty d_{σ} orbital on the metal center augmented by a weaker back-donation, **2b**, of metal d_{π} electrons to the dihydrogen σ^* orbital. The back-donation, **2b**, stabilizes the side-on H₂ coordination mode, and might lead to a complete cleavage of the H–H bond if the electron transfer is too large. Thus, the balance between the nonclassical dihydrogen isomer and the classical hydride tautomer, **2c**, is to a large extent controlled by the back-donation **2b**.



In this section, we carry out an extended transition state (ETS) analysis on the M–H₂ bond in $M(\text{PH}_3)_3\text{H}_4$, see Table 4. By decomposing the M–H₂ bond energy into several parts, we are able to distinguish the donation and back-donation interactions quantitatively. A similar analysis based on the ETS scheme has been reported briefly by Bickelhaupt *et al.*²⁶ for $\text{Cr}(\text{CO})_5\text{H}_2$ and PtCl_4H_2 . A related energy decomposition analysis was also used by Maseras *et al.*^{5p} for $\text{Os}(\text{PH}_3)_3\text{H}_4$.

According to the ETS method,²⁷ the bond energy between H₂ and metal fragment $M(\text{PH}_3)_3\text{H}_2$ can be decomposed as:

$$\Delta E = -[E_{\text{steric}} + E_{\text{prep}} + E_{\text{orb}}] \quad (1)$$

Here E_{steric} represents the steric interaction energy between the fragments $M(\text{PH}_3)_3\text{H}_2$ and H₂. This term is made up of the stabilizing electrostatic interaction between the two fragments as well as the repulsive two-orbital-four-electron interactions between occupied orbitals on the two fragments. The total contribution from E_{steric} to the M–H₂ bond energy, Table 4, is destabilizing and obtained from a calculation on $M(\text{PH}_3)_3\text{H}_4$ in which only the occupied orbitals of $M(\text{PH}_3)_3\text{H}_2$ and H₂ are involved. The contribution to the M–H₂ bond energy from E_{steric} amounts to between 17 and 25 kcal/mol, Table 4.

The term E_{prep} comes from the energy required to relax the structures of the free fragments to the geometries they take up in the combined molecule. The main contributor is the stretch of the H₂ molecule from 0.741 Å in free H₂ to between 0.8 and 1.0 Å in the dihydrogen complexes **1b** and **1c** corresponding to a E_{prep} contribution of between 30 and 18 kcal/mol. We shall for comparison also consider the dihydride **1a** as formed from $M(\text{PH}_3)_3\text{H}_2$ and H₂ stretched to the dissociation limit. In this case E_{prep} is close to 100 kcal/mol, Table 4.

The last term, E_{orb} , is due to orbital interactions between empty and occupied fragment orbitals, and it represents the stabilizing component of ΔE in eq 1. The E_{orb} term can be further separated as:

$$E_{\text{orb}} = E_{\text{D}} + E_{\text{BD}} + E_{\text{syn}} + E_{\text{res}} \quad (2)$$

Here E_{D} is the contribution from the σ -donation, **2a**, obtained as the stabilization gained by adding the unoccupied d_{σ} acceptor orbital to the set of occupied fragment orbitals in a calculation on $M(\text{PH}_3)_3\text{H}_4$. Likewise E_{BD} representing the corresponding back-donation, **2b**, is obtained from a calculation with σ^* as the only added virtual fragment orbital. Finally, the synergic energy term E_{syn} is determined as the extra stabilization gained in addition to $E_{\text{BD}} + E_{\text{D}}$ by having both d_{σ} and σ^* included.

The rest or residual parts of the bonding interactions of E_{orb} are combined in E_{res} . The residual term E_{res} arises primarily from a polarization of the electron density in order to alleviate the repulsive interaction between occupied orbitals contained in E_{steric} . We note that the contributions from E_{res} and E_{steric} to a large extent cancel in the combined expression for ΔE in eq

(26) Bickelhaupt, F. M.; Baerends, E. J.; Ravenek, W. *Inorg. Chem.* **1990**, 29, 350.

(27) (a) Ziegler, T.; Rauk, A. *Theor. Chim. Acta* **1977**, 46, 1. (b) Baerends, E. J.; Rozendaal, A. *NATO ASI* **1986**, C176, 159. (c) Ziegler, T. *NATO ASI* **1992**, C378, 367. (d) Kraatz, H.-B.; Jacobsen, H.; Ziegler, T.; Boorman, P. M. *Organometallics* **1993**, 12, 76.

1, Table 4. We shall in the following primarily base our discussion on E_D and E_{BD} .

For the nonclassical dihydrogen isomers **1c** and **1b**, one striking feature in Table 4 is that the $-E_{BD}$ term is comparable to or even larger than the $-E_D$ contribution. Since our calculated H1–H2 bond distances for the **1b** and **1c** isomer appear to be at the upper end of what is observed experimentally for dihydrogen complexes, and we only extract the $-E_D$ and $-E_{BD}$ contributions from the one-to-one frontier orbital interactions, we cannot exclude the possibility that the back-donation contribution is overestimated in this calculation. However, it is likely that back-donation, **2b**, plays a role comparable to that of the donation, **2a**, for the stability of the M–H₂ bond.

Experimentally, inelastic neutron scattering (INS) technique can be used to determine the energy barrier to rotation for the H₂ ligand.²⁸ The height of the barrier²⁹ provides in turn a measure for the degree of back-donation since **2b**, but not **2a**, should be influenced by the orientation of H₂. It has been concluded by Kubas *et al.*^{29b} that back-donation is more of a factor than σ -bonding in influencing the stability, H–H distance, and possibly overall M–H₂ bond strengths in dihydrogen complexes. Furthermore, the periodic trend of the back-donation was found to decrease down the group 6 triad Cr, Mo, W for the complexes M(CO)₃(PR₃)₃(H₂),^{29b} based on the H₂ rotation barrier determined by INS techniques. It is very interesting to note that the $-E_{BD}$ contribution in Table 4 also shows such a periodic trend for each of the two isomers **1b** and **1c**.

There are no experimental M–H₂ bond energy data available for M(PR₃)₃H₄. Our calculated values for the **1b** isomer with M = Fe and Ru are 26 and 31 kcal/mol, respectively. These values are larger than the experimental estimate of 25 kcal/mol for W(CO)₃(PCy)₂-H₂³⁰ and 17 kcal/mol for Cr(CO)₅-H₂,³⁰ based on photoacoustic calorimetry and kinetic measurement.

The most relevant information in Table 4 for the classical hydrides **1a** is the average M–H bond energies $D(M-H)_{av}$. We find an increase in the M–H bond energy down the iron triad with $D(Fe-H)_{av} = 69.9$ kcal/mol, $D(Ru-H)_{av} = 71.5$ kcal/mol, and $D(Os-H)_{av} = 72.2$ kcal/mol for the relativistic calculations. This is in the range of a typical M–H bond strength³¹ and also not so far from the average W–H bond strength for the dihydride isomer of W(PR₃)₂(CO)₃H₂, 65 ± 6 kcal/mol, as estimated by Gonzalez *et al.*³² We note further for osmium an increase of 6.9 kcal/mol in the average Os–H bond strength due to relativistic effects.

We shall now turn to a discussion of how relativistic effects are able to induce a preference for the classical hydride **1a** in the case of osmium whereas the lighter congeners iron and ruthenium, for which relativistic effects are less important, prefer the dihydrogen conformation **1b**. Table 4 affords to this end a full ETS decomposition of ΔE for all three isomers **1a–1c** of Os(PH₃)₃H₄ in the nonrelativistic (NL-SCF) as well as relativistic (NL-SCF+QR) case. Again, ΔE represents the energy of formation of Os(PH₃)₃H₄, whether it is classical or nonclassical, from H₂ and Os(PH₃)₃H₂. For the hydride, **1a**, the preparation energy, $-E_{prep}$, is large (~100 kcal/mol) since the H₂ unit is near the dissociation limit. Further, the average Os–H dis-

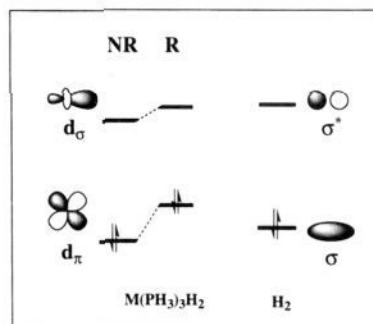


Figure 2. The relativistic influence on the d_σ donor orbital and d_π acceptor orbital of the Os(PH₃)₂(H₂) fragment.

sociation energy, $D(Os-H)_{av}$, for the dihydride is related to ΔE of **1a** by

$$D(Os-H)_{av} = \frac{1}{2}[\Delta E + E_c(H-H)] \quad (3)$$

where the electronic dissociation energy $E_c(H-H)$ of H₂ is calculated as 112.9 kcal/mol.

We note at the outset that relativity stabilizes all three isomers **1a–1c** compared to H₂ and Os(PH₃)₃H₂. The first stabilizing factor is the reduction in the steric interaction energy E_{steric} . This is a direct result of a decrease in the kinetic energy induced by the mass-velocity correction, as discussed in detail by Ziegler *et al.* elsewhere.³³ The second stabilizing factor is the increase in the back-donation contribution $-E_{BD}$, to some degree offset by a reduction in the donation energy contribution $-E_D$, Table 4.

The impact of relativity on $-E_{BD}$ and $-E_D$ can be understood by looking at the relativistic changes in the energies of the osmium-based acceptor orbital d_σ , **2a**, and donor orbital d_π , **2b**. It follows from Figure 2 that both d-based orbitals are raised in energy by relativity. The energy increase for d_π will enhance back-donation since this orbital now is closer to σ^* in energy. On the other hand, the energy increase for d_σ will reduce donation since the gap to σ of H₂ is larger. The relativistic increase in the energy of the osmium d orbitals is the result³⁴ of a relativistic contraction of the s and p core orbitals, which in turn reduces the effective nuclear charge experienced by electrons in the 5d shell on osmium. It should be pointed out that the contraction of the s and p core orbitals again is caused by a reduction of their kinetic energy induced by the mass-velocity correction.^{33,34}

It follows from Table 4 that relativity increases $-E_{BD}$ and decreases $-E_D$ for all three conformations **1a–1c** as the relativistic destabilization of the 5d orbital makes osmium a stronger donor. It is further seen from Table 4 that the relativistic increase in metal donor ability shifts the equilibrium, **2c**, toward the dihydride isomer **1a**, just as the substitution of a ligand L in the dihydrogen L_nM-H_2 complex by a stronger donor L' might produce the dihydride $L_{n-1}L'M(H)_2$.

IV. Conclusion

By using the current density functional method at the NL-SCF+QR level with nonlocal and quasirelativistic corrections included self-consistently, we are able to reproduce the experimental order of relative stabilities for classical and nonclassical isomers of M(PH₃)₃H₄ with M = Fe, Ru, Os. We found that

(33) (a) Ziegler, T.; Snijders, J. G.; Baerends, E. J. *Chem. Phys. Lett.* **1980**, *75*, 1. (b) Ziegler, T.; Snijders, J. G.; Baerends, E. J.; Ros, P. J. *Chem. Phys.* **1981**, *74*, 1271.

(34) (a) Pyykkö, Declaux, J.-P. *Acc. Chem. Res.* **1979**, *12*, 276. (b) Schwarz, W. H. E.; van Wezenbeek, E. M.; Baerends, E. J.; Snijders, J. G. *J. Phys. B* **1989**, *22*, 1515.

(28) Eckert, J. *Spectrochim. Acta* **1992**, *48A*, 363.

(29) (a) Eckert, J.; Kubas, G. J.; Hall, J. H.; Hay, P. J.; Boyle, C. M. *J. Am. Chem. Soc.* **1990**, *112*, 2324. (b) Kubas, G. J.; Nelson, J. E.; Bryan, J. C.; Eckert, J.; Wisniewski, L.; Zilm, K. *Inorg. Chem.* **1994**, *33*, 2954.

(30) Data as quoted in ref 1e.

(31) Simoes, J. A. M.; Beauchamp, J. L. *Chem. Rev.* **1990**, *90*, 629.

(32) Gonzalez, A. A.; Zhang, K.; Mukerjee, S. L.; Hoff, C. D.; Khalsa, G. R.; Kubas, G. J. In *Bonding energetics in organometallic compounds*; ACS Symposium Series 428; Marks, T. J., Ed.; American Chemical Society: Washington, DC, 1990.

the most stable isomer is a nonclassical dihydrogen complex for Fe and Ru but a classical hydride for Os. We are further able to demonstrate that this changeover is the result of a relativistic destabilization of the osmium 5d orbitals which makes the metal center a stronger donor. We have previously shown that the same relativistic destabilization of the 5d orbital increases the bond strength between a heavy transition metal center and π -ligands such as CO, O₂, C₂H₂, C₂H₄, and CH₂.⁹ All these effects are ultimately caused by the relativistic mass increase of electrons moving with high instantaneous velocities near the nuclei.³³

Acknowledgment. This investigation was supported by the Natural Sciences and Engineering Research Council of Canada (NSERC) as well as the donors of the Petroleum Research Fund, administered by the American Chemical Society (ACS-PRF No. 27023-AC23). J.L. thanks NSERC for an International Fellowship and Professor P. Pyykkö (University of Helsinki) for correspondence. The Academic Computing Services of the University of Calgary is acknowledged for access to the IBM-RISC/System 6000 facilities.

JA944190N